

# Detection of High Impedance Faults in Microgrids using Machine Learning

Pallav Kumar Bera  
School of Engr. & Computer Science  
University of Evansville  
Indiana, USA  
pb141@evansville.edu

Vajendra Kumar  
Dept. of Electrical Engineering  
IIT Roorkee, India,  
kumarvajendra@gmail.com

Samita Rani Pani  
School of Electrical Engineering  
VSSUT, Burla, India  
KIIT Deemed to be University, India  
samita.panifel@kiit.ac.in

Vivek Bargate  
Dept. of Electrical Engineering  
NIT Raipur, India  
vicky30786@gmail.com



**Abstract**—This article presents differential protection of the distribution line connecting a wind farm in a microgrid. Machine Learning (ML) based models are built using differential features extracted from currents at both ends of the line to assist in relaying decisions. Wavelet coefficients obtained after feature selection from an extensive list of features are used to train the classifiers. Internal faults are distinguished from external faults with CT saturation. The internal faults include the high impedance faults (HIFs) which have very low currents and test the dependability of the conventional relays. The faults are simulated in a 5-bus system in PSCAD/EMTDC. The results show that ML-based models can effectively distinguish faults and other transients and help maintain security and dependability of the microgrid operation.

**Index Terms**—Microgrid, High Impedance Faults, Machine Learning, Differential Protection

## I. INTRODUCTION

Microgrids have gathered much attention in the past decade due to the advances in distributed generation (DG) development. Microgrid reduces distribution losses, provides generation at the consumption sites, and are more reliable. However, protection of microgrids challenges the conventional relays. The fault current in a microgrid varies depending on the type of DG, operating conditions, and network topology. As a result, traditional overcurrent relays become unreliable [1]. If the faults are high impedance faults (HIFs), the issue becomes even more complex. HIFs that occur in distribution networks are too small in magnitude that they often bypass the conventional relays without getting detected [2]. The energized conductors in contact with the ground surface are dangerous for animal and plant life and cause losses. HIFs are common and the

growth and need for distributed generations will only augment the occurrence of such low current faults [3]. Hence, a reliable and fast protection system is necessary.

Several strategies for detecting HIFs in distribution networks have been proposed by researchers. Mathematical morphology which extracts information from voltage and current was used in [4]. To detect the low currents associated with HIFs; even, odd, and inter-harmonics in the fault current were used in [5]–[7]. Genetic algorithm and wavelet transforms were used in [8] and [9] respectively. Use of Machine Learning (ML) algorithms namely Neural Networks [10], Decision Tree [11], Support Vector Machines [12], k-Nearest Neighbor [13], Naive Bayes [14] have also been considered. Expert systems have also proven their worth for fault detection and classification in microgrids. An intelligent fault detection scheme for microgrid systems based on wavelet transform and deep learning was proposed in [15]. Wavelet transform and decision tree were used for the protection of microgrids with inverter interfaced DGs in [16]. Predictive analytics has also been used to differentiate internal faults and magnetizing inrush in [17]. Feature-based distance protection was proposed in [18] for the protection of transmission lines connected to wind farms. This work suggests a comprehensive microgrid protection taking into account various operating modes, including islanded and grid-connected.

There are five sections to the paper. The literature review and overview of this paper are included in Section I. The test system and the creation of the HIF model in PSCAD/EMTDC are described in Section II. The feature extraction and selection are demonstrated in Section III. The findings of this methodology are described in Section IV. Finally, in Section V, conclusions are drawn.

© 2022 IEEE. Personal use of this material is permitted. Permission from IEEE must be obtained for all other uses, in any current or future media, including reprinting/republishing this material for advertising or promotional purposes, creating new collective works, for resale or redistribution to servers or lists, or reuse of any copyrighted component of this work in other works

To appear in IEEE Green Energy and Smart Systems Conference, Long Beach, CA

TABLE I: Parameters of the Microgrid under study

System	Parameters
Main Grid (G)	Frequency: 60Hz, Rated Voltage: 230 kV
Distributed Generations: DG2 (Diesel Generator):	Rated Power:2MW, Rated line voltage:13.8kV & rated RMS line current: 0.833 kA
DG3 (PV)	Rated Power:0.25MW, at 1000W/m <sup>2</sup> & nominal temperature of 28 <sup>0</sup> C
DG4 (Wind Farm)	Rated Power: 2.5MW, Wind Speed: 11m/s
Distribution Lines:	
T21	10 km
T23	20 km
T24	30 km
T45	10 km
Transformers:	
T1	230kV/ 20kV, 100 MVA
T2	13.86 kV/ 20kV, 3MVA
T3	460V/ 20kV, 1MVA
T4	690V/ 20kV, 5.5 MVA
Loads:	
L1	0.95 MW, 0.475 MVAR
L2	0.95 MW, 0.475 MVAR
L3	0.05 MW, 0.025 MVAR
L5	0.95 MW, 0.475 MVAR

## II. MODELING

This section describes the microgrid under study, the modeling of HIF, and power system events simulated in PSCAD/EMTDC considered for the feature extraction and classification.

### A. System Studied

The microgrid system under study is shown in Fig. 1. The 5-bus microgrid consists of a Diesel Generator (DG2), PV (DG3), and a Wind Farm (DG4). A DC-DC converter is connected to the PV array. The PV array's output is determined by irradiance and temperature. The converter adjusts the dc-link current based on the power generated by the maximum power point tracker. The dc voltage is controlled by the voltage source converter. The type-3 wind turbine generator has mechanical and electrical components. The wind turbine extracts the most power possible from the available wind, while the electrical system transforms mechanical energy into electrical energy. It consists of the induction machine and the AC-DC-AC converter. The governor, IC engine, and synchronous machine are the primary components of a diesel generator. The details of the distributed generation are given in Table I.

### B. HIF Modeling

There are three primary ways to model HIFs [19]. Out of these, the one where two- anti-parallel DC sources are connected via two diodes and two variable resistors is used in this paper. The HIF model used in this paper is shown in Fig. 2. The two variable resistors model the dynamic arc, and the

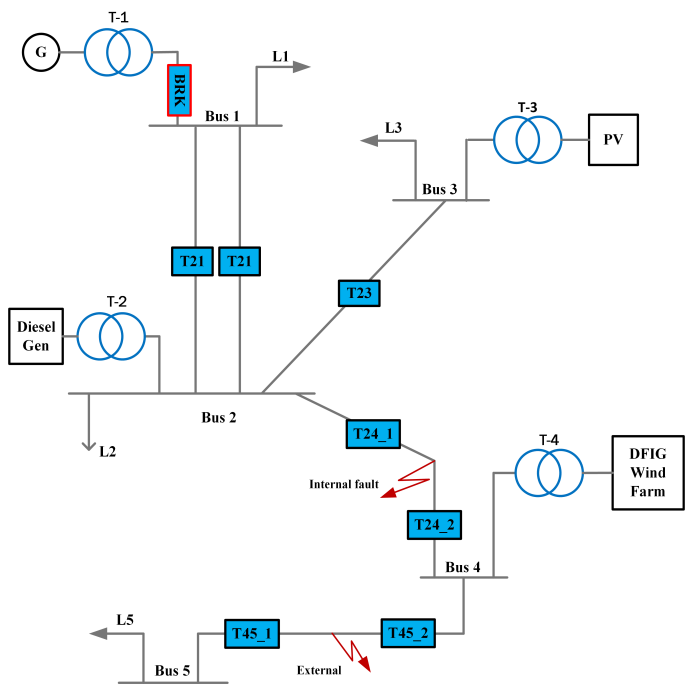


Fig. 1: 5-bus Test System.

varying DC sources model the asymmetry in the fault currents. In the positive half cycle  $V_{ph} > V_p$ , in the negative half cycle  $V_{ph} < V_n$ , and when  $V_n < V_{ph} < V_p$  current is zero.

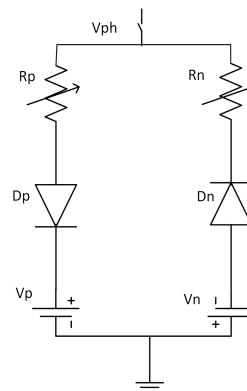


Fig. 2: High Impedance Fault model

### C. Power System Events

The distribution line T24 between bus-2 and bus-4 is considered for simulating the internal faults which include the HIFs. Type 1 internal faults include LG, LLG, LL, LLLG, and LLL faults, whereas Type 2 internal faults, also referred to as the HIFs, are the downed conductor faults for each phase. Tables II, III, and IV show the parameters (fault type, fault resistance, fault inception angle, etc.), their values, and the number of cases simulated for the fault data in grid-connected

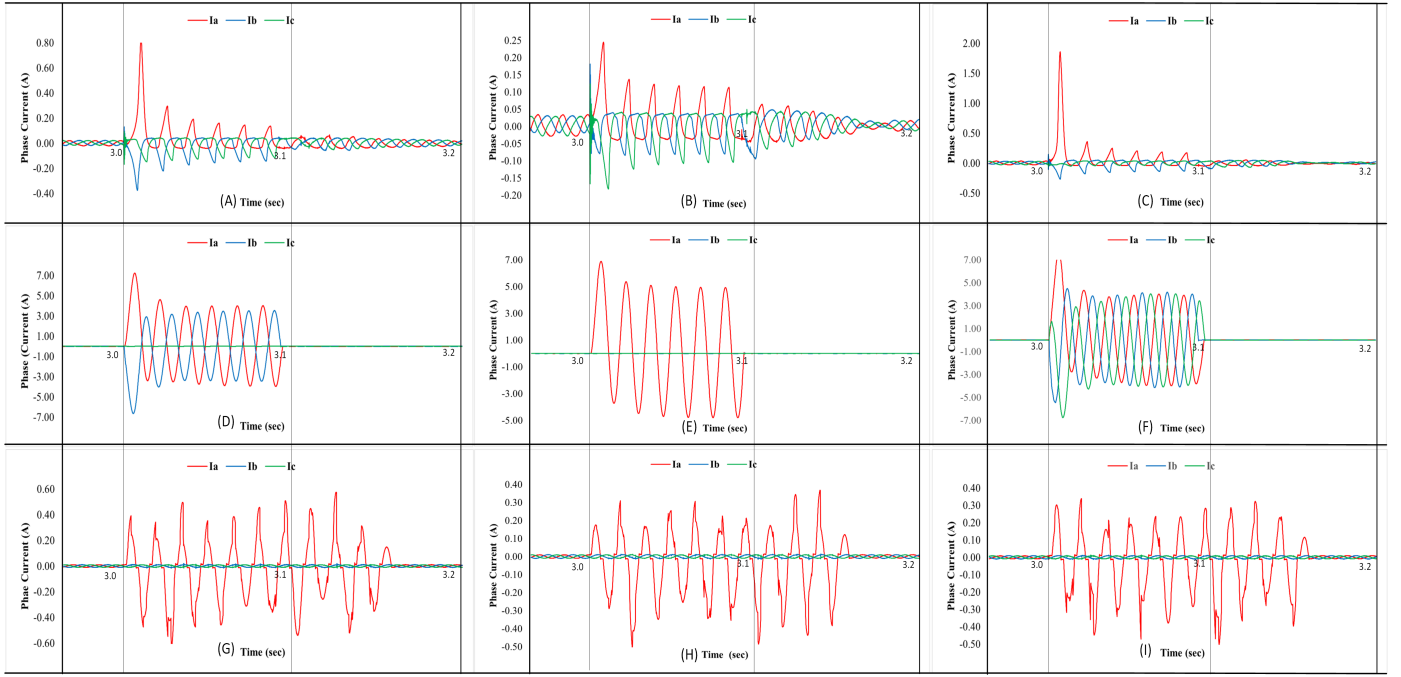


Fig. 3: External faults with CT saturation (A,B,C), internal faults (D,E,F), and HIF faults (G,H,I)

TABLE II: Parameters for External faults

Parameter & Values	Operating condition cases	
	Grid Connected	Islanded
Fault Type (LG, LLG, LL, LLLG, LLL)	5	5
Fault Resistance (0.01, 0.1, 1, 10 $\Omega$ s)	4	4
Fault Inception Angle (between $0^\circ$ - $360^\circ$ )	10	10
Balanced/Unbalanced/Low Voltage	2	3
Total cases	400	600

TABLE III: Parameters for Internal faults (Non-HIFs)

Parameter & Values	Operating condition cases	
	Grid Connected	Islanded
Fault Type (LG, LLG, LL, LLLG, LLL)	5	5
Fault Resistance (0.01, 0.1, 1, 10, 20 $\Omega$ s)	5	5
Fault Inception Angle (between $0^\circ$ - $360^\circ$ )	7	7
Balanced/Unbalanced/Low voltage	2	3
Total cases	350	525

TABLE IV: Parameters for HIF faults

Parameter & Values	Operating condition cases	
	Grid Connected	Islanded
Fault Type (LG)	1	1
Phases (a,b, and c)	3	3
Fault Time	20	20
Balanced/Unbalanced/Low voltage	2	3
Total cases	120	180

TABLE V: Events in the Microgrid

Event	Event Type	No. of Cases
Internal Faults	Type 1 (Non-HIFs)	875
	Type 2 (HIFs)	300
External Faults	with CT saturation	1000

and islanded modes. For internal and external faults, balanced and unbalanced loads with LG, LLG, LL, LLL, and LLLG fault types are evaluated, whereas only LG faults in the three phases for HIFs are considered. For HIFs the fault impedance is varied between  $50 \Omega$  to  $300 \Omega$  randomly in the interval of 0.2ms during fault. Lower voltages up to 0.9 per unit are also taken into account while simulating the faults [20]. The external faults are simulated in line T45 while the CTs at the two ends of line T24 were burdened differently. Fig. 3 shows the 3-phase

differential currents for external faults with CT saturation, internal faults, and high impedance faults. (A), (B), and (C) show external faults with CT saturation; (D), (E), and (F) show internal Type 1 faults; and (G), (H), and (I) show internal Type 2 faults in grid-connected, islanded, low voltage condition, balanced and unbalanced loading conditions. Table V shows the number of internal faults and external faults simulated in the microgrid. Using the parameters mentioned above, 1175 internal faults and 1000 external faults are generated.

TABLE VI: Hyperparameter Selection

Classifier	Hyperparameter grid	Best Hyperparameters
Decision Tree	<b>criterion:</b> entropy,gini	<b>criterion:</b> entropy
Random Forest	<b>max_depth:</b> 4-20, <b>max_features:</b> 0.1-1, <b>min_samples_leaf:</b> 5-60, <b>estimators:</b> 500-4000	<b>max_depth:</b> 5, <b>max_features:</b> 0.1, <b>min_samples_leaf:</b> 5, <b>estimators:</b> 500
Gradient Boost	<b>learning_rate:</b> 0.01-0.1, <b>max_depth:</b> 4-20, <b>estimators:</b> 500-4000, <b>subsample:</b> 0.5-1	<b>learning_rate:</b> 0.01, <b>max_depth:</b> 5, <b>estimators:</b> 500, <b>subsample:</b> 0.5
Multi Layer Perceptron	<b>activation:</b> logistic, identity, tanh, relu, <b>alpha:</b> 0.0001-0.01, <b>hidden_layer:</b> (30-100, 8-30), <b>learning_rate:</b> adaptive, <b>solver:</b> lbfgs, adam, sgd	<b>activation:</b> logistic, <b>alpha:</b> 0.0001, <b>hidden_layer:</b> (88, 23), <b>learning_rate:</b> adaptive, <b>solver:</b> lbfgs
Naive Bayes	-	-
K-Nearest Neighbor	<b>leaf_size:</b> 2-15, <b>neighbors:</b> 3-10, <b>distance:</b> manhattan, euclidean	<b>leaf_size:</b> 3, <b>neighbors:</b> 4, <b>distance:</b> manhattan
Support Vector Machine	<b>C:</b> 0.1-1000, <b>gamma:</b> 0.0001-1, <b>kernel:</b> rbf, poly	<b>C:</b> 1000, <b>gamma:</b> 1, <b>kernel:</b> rbf

### III. FEATURE EXTRACTION AND SELECTION

Feature selection helps identify key characteristics in the differential currents. The selection of informative, discriminating, and independent features is a critical component in pattern recognition and classification tasks. It also helps to reduce the input matrix size and thus increases the credibility of the model. In [21]–[23] several time, time-frequency, and frequency domain features were extracted and then selected to detect and classify power system events like faults and transients. Here, the importance of individual features is calculated in terms of information gain. The features with higher information gain are more relevant in classifying the faults and non-fault events.

The features which can be spectral (FFT coeff. etc.), time-frequency (wavelet coeff.), information theory (entropy, approximate entropy, etc.), or statistical (autocorrelation, minimum, maximum, mean, median, etc.) are calculated in Python. The list of features is detailed in [24]. 2289 features are examined and then the topmost features from the 3-phase differential currents obtained via the CTs at both ends are used to train the classifier models. Thus, Continuous Wavelet coefficients are obtained in the feature selection process.

#### A. Continuous Wavelet Transform

The Mexican Hat wavelet,  $\psi(t, p, q)$  is obtained by scaling and shifting the mother wavelet  $\psi(t)$

$$\psi(t, p, q) = \frac{2}{\sqrt{3p\pi^{\frac{1}{4}}}} \left(1 - \frac{(t-q)^2}{p^2}\right) \exp\left(-\frac{(t-q)^2}{2p^2}\right) \quad (1)$$

where  $p$  and  $q$  are the scaling and shifting parameters.

The Continuous Wavelet Transform (CWT) of a signal  $y(t)$  is then obtained by using

$$Y(y(t), p, q, \psi(t)) = \int_{-\infty}^{+\infty} y(t)\psi^*(t, p, q)dt \quad (2)$$

where  $\psi^*(t, p, q)$  is the complex conjugate of  $\psi(t, p, q)$

TABLE VII: Model Performance

Classifier	Balanced Accuracy	Dependability	Security
Decision Tree	99.68%	99.72%	99.64%
Random Forest	99.23%	99.17%	99.29%
Gradient Boost	99.68%	99.72%	99.64%
Multi Layer Perceptron	99.85%	99.7%	100%
Naive Bayes	56.3%	12.6%	100%
K-Nearest Neighbor	99.86%	99.72%	100%
Support Vector Machine	100%	100%	100%

### IV. RESULTS

The balanced accuracy (eq.3) which is a better representation of accuracy is obtained for all the classifiers considered in the study. Eq. 4 is used to calculate the dependability for internal faults, which includes HIF faults, and eq. 5 is used to calculate the security for external faults with CT saturation.

$$\bar{\eta} = \frac{1}{2} \left( \frac{TP}{TP + FN} + \frac{TN}{TN + FP} \right) \quad (3)$$

$$Dependability = \left( \frac{TP}{TP + FN} \right) \quad (4)$$

$$Security = \left( \frac{TN}{TN + FP} \right) \quad (5)$$

Here, TP is true positive, TN is true negative, FP is false positive, and FN is false negative. The classifier models used to differentiate the internal faults and external faults are: Decision Tree, Random Forest, Gradient Boost, K-Nearest Neighbor, Naive Bayes, Support Vector Machine, and Multi Layer Perceptron. It is critical to find the optimal hyperparameters (parameter that affects how the learning process is carried out) for these algorithms. It fine-tunes the parameters and minimizes the loss function. The hyperparameters are optimized using grid search over possible values of the individual parameter. Table VI shows the hyperparameter grid and the best choice for testing the different classifiers considered in this study. Cross-validation is used to avoid overfitting and to credibly measure the merit of the prediction. The classification results are given

in Table VII. The Wavelet transform coefficients obtained from the external and internal faults simulated in Section II are used for training and testing the seven classifiers. On this fault data, all classifiers except Naive Bayes fared well, with Support Vector Machine outperforming the others.

## V. CONCLUSION

The paper presents differential protection of lines connecting a wind farm in a microgrid. The differential features obtained from the currents at both ends of the line under consideration are used to build the ML-based models. 2175 external and internal faults conditions are simulated by varying different system parameters. The findings suggest that models based on ML can successfully differentiate internal and external faults. The performance of the ML algorithms is analyzed in the presence of high impedance faults. ML-based fault detection is able to identify internal and external faults with CT saturation even in the face of these low-magnitude current faults.

## REFERENCES

- [1] S. Kar, S. R. Samantaray, and M. D. Zadeh, "Data-mining model based intelligent differential microgrid protection scheme," *IEEE Systems Journal*, vol. 11, no. 2, pp. 1161–1169, 2017.
- [2] C. Benner and B. Russell, "Practical high-impedance fault detection on distribution feeders," *IEEE Transactions on Industry Applications*, vol. 33, no. 3, pp. 635–640, 1997.
- [3] M. G. Adamiak, C. Wester, and M. Thakur, "High impedance fault detection on distribution feeders," 2001.
- [4] M. Kavi, Y. Mishra, and M. D. Vilathgamuwa, "High-impedance fault detection and classification in power system distribution networks using morphological fault detector algorithm," *IET Generation, Transmission & Distribution*, vol. 12, pp. 3699–3710(11), August 2018.
- [5] D. Yu and S. Khan, "An adaptive high and low impedance fault detection method," *IEEE Transactions on Power Delivery*, vol. 9, no. 4, pp. 1812–1821, 1994.
- [6] W. H. Kwon, G. W. Lee, Y. M. Park, M. C. Yoon, and M. H. Yoo, "High impedance fault detection utilizing incremental variance of normalized even order harmonic power," *IEEE Transactions on Power Delivery*, vol. 6, no. 2, pp. 557–564, 1991.
- [7] J. R. Macedo, J. W. Resende, C. A. J. Bissochi, D. Carvalho, and F. C. Castro, "Proposition of an interharmonic-based methodology for high-impedance fault detection in distribution systems," *IET Generation, Transmission & Distribution*, vol. 9, pp. 2593–2601(8), December 2015.
- [8] M.-R. Haghifam, A.-R. Sedighi, and O. Malik, "Development of a fuzzy inference system based on genetic algorithm for high-impedance fault detection," *IEE Proceedings - Generation, Transmission and Distribution*, vol. 153, pp. 359–367(8), May 2006.
- [9] N. I. Elkalashy, M. Lehtonen, H. A. Darwish, A.-M. I. Taalab, and M. A. Izzularab, "Dwt-based detection and transient power direction-based location of high-impedance faults due to leaning trees in unearthened mv networks," *IEEE Transactions on Power Delivery*, vol. 23, no. 1, pp. 94–101, 2008.
- [10] C. Kim and B. Russell, "A learning method for use in intelligent computer relays for high impedance faults," *IEEE Transactions on Power Delivery*, vol. 6, no. 1, pp. 109–115, 1991.
- [11] Y. Sheng and S. Rovnyak, "Decision tree-based methodology for high impedance fault detection," *IEEE Transactions on Power Delivery*, vol. 19, no. 2, pp. 533–536, 2004.
- [12] M. Sarlak and S. M. Shahrtash, "High-impedance faulted branch identification using magnetic-field signature analysis," *IEEE Transactions on Power Delivery*, vol. 28, no. 1, pp. 67–74, 2013.
- [13] T. Lai, L. Snider, E. Lo, and D. Sutanto, "High-impedance fault detection using discrete wavelet transform and frequency range and rms conversion," *IEEE Transactions on Power Delivery*, vol. 20, no. 1, pp. 397–407, 2005.
- [14] A.-R. Sedighi, M.-R. Haghifam, O. Malik, and M.-H. Ghassemian, "High impedance fault detection based on wavelet transform and statistical pattern recognition," *IEEE Transactions on Power Delivery*, vol. 20, no. 4, pp. 2414–2421, 2005.
- [15] J. J. Q. Yu, Y. Hou, A. Y. S. Lam, and V. O. K. Li, "Intelligent fault detection scheme for microgrids with wavelet-based deep neural networks," *IEEE Transactions on Smart Grid*, vol. 10, no. 2, pp. 1694–1703, 2019.
- [16] D. P. Mishra, S. R. Samantaray, and G. Joos, "A combined wavelet and data-mining based intelligent protection scheme for microgrid," *IEEE Transactions on Smart Grid*, vol. 7, no. 5, pp. 2295–2304, 2016.
- [17] S. R. Pani, P. K. Bera, and V. Kumar, "Detection and classification of internal faults in power transformers using tree based classifiers," in *2020 IEEE International Conference on Power Electronics, Drives and Energy Systems (PEDES)*, pp. 1–6, 2020.
- [18] P. K. Bera, V. Kumar, and C. Isik, "Distance protection of transmission lines connected to type-3 wind farms," in *2021 IEEE Power and Energy Conference at Illinois (PECI)*, pp. 1–7, 2021.
- [19] Q. Cui, K. El-Arroudi, and Y. Weng, "A feature selection method for high impedance fault detection," *IEEE Transactions on Power Delivery*, vol. 34, no. 3, pp. 1203–1215, 2019.
- [20] A. Hooshyar and R. Iravani, "A new directional element for microgrid protection," *IEEE Transactions on Smart Grid*, vol. 9, no. 6, pp. 6862–6876, 2018.
- [21] P. K. Bera and C. Isik, "Identification of stable and unstable power swings using pattern recognition," in *2021 IEEE Green Technologies Conference (GreenTech)*, pp. 286–291, 2021.
- [22] P. K. Bera, C. Isik, and V. Kumar, "Discrimination of internal faults and other transients in an interconnected system with power transformers and phase angle regulators," *IEEE Systems Journal*, vol. 15, no. 3, pp. 3450–3461, 2021.
- [23] P. K. Bera and C. Isik, "A data mining based protection and classification of transients for two-core symmetric phase angle regulators," *IEEE Access*, vol. 9, pp. 72937–72948, 2021.
- [24] M. Christ, N. Braun, J. Neuffer, and A. W. Kempa-Liehr, "Time series feature extraction on basis of scalable hypothesis tests (tsfresh – a python package)," *Neurocomputing*, 2018.